Journal of Molecular Spectroscopy 391 (2023) 111732

Contents lists available at ScienceDirect

Journal of Molecular Spectroscopy

journal homepage: www.elsevier.com/locate/yjmsp

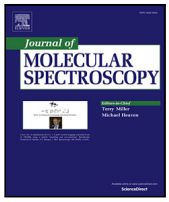

MARVEL analysis of high-resolution spectra of thioformaldehyde (H_2CS)

Thomas M. Mellor[1], Alec Owens[1], Jonathan Tennyson[1], Sergei N. Yurchenko [*,1]

Department of Physics and Astronomy, University College London, Gower Street, WC1E 6BT London, United Kingdom

ARTICLE INFO

Keywords:
Molecular data
Potential energy surface
Line lists
Radiative transfer
Databases
ExoMol

ABSTRACT

We present a comprehensive analysis of the published spectroscopic literature on the main isotopologue of thioformaldehyde ($^1H_2{}^{12}C^{32}S$). All reliable experimental transitions from publications over the last 42 years have been extracted and compiled into a consistent dataset with unique quantum number labelling and measurement uncertainties. The dataset covers the ground, ν_1, ν_2, ν_3, ν_4, ν_5, ν_6, and $2\nu_2$ vibrational bands of H_2CS. The ν_4 and ν_6 modes have very close band centres and consequently different data sources had incompatible vibrational assignments. Variational calculations are used as a basis to assign vibrational states of the associated transitions consistently. The transitions could then be processed using the robust MARVEL (Measured Active Rotational-Vibrational Energy Levels) procedure to produce a highly accurate set of 4254 rotation-vibration energy levels up to $J = 54$ and $3729\,cm^{-1}$. The resulting set of labelled empirical-quality energies will be of significant use in the production of a hot molecular line list of H_2CS, as well as other spectroscopic and radiative applications given the astrophysical importance of thioformaldehyde.

1. Introduction

Thioformaldehyde (main isotopologue $^1H_2{}^{12}C^{32}S$, henceforth referred to as H_2CS) is an abundant astrophysical molecule that has been the subject of numerous spectroscopic studies since its original interstellar detection [1]. It has been detected in nearby [2,3] and more distant galaxies [4], molecular clouds [5], in the comet Hale-Bopp [6], which was the first detection of H_2CS in any comet, as well as being efficiently formed in massive star-forming regions such as Sagittarius B2 through bimolecular reactions [7]. As a simple organosulphur molecule, H_2CS is likely to occur in many other astronomical environments, notably in exoplanets where sulphur chemistry can significantly influence the atmospheric composition [8,9].

There have been a number of studies of the rotation-vibration (ro-vibrational) spectrum of H_2CS. On the theoretical side, an *ab initio* room-temperature line list for H_2CS was generated with a high-level of theory (CCSD(T)-F12b) with large F12-optimised correlation consistent basis sets and considered additional small energy corrections accounting for core-valence electron correlation, higher-order coupled cluster terms, scalar relativistic effects and diagonal Born-Oppenheimer corrections [10]. Benchmark calculations of the ro-vibrational spectrum of H_2CS were performed using a newly computed *ab initio* potential energy surface (PES) and dipole moment surface (DMS) [11]. The ro-vibrational calculations showcased a fully automated "black-box"-type procedure employing vibrational self-consistent field and vibrational configuration interaction theory based on the Watson Hamiltonian. Intramolecular vibrational-energy redistribution between different states of H_2CS was explored using the multiconfiguration time-dependent Hartree (MCTDH) method [12]. This work employed an empirically-refined quartic force field [13] (based on an *ab initio* anharmonic force field [14]) and *ab initio* DMS from density functional theory (DFT) calculations [15]. These surfaces were also utilised in more rigorous variational calculations of the ro-vibrational spectrum of H_2CS up to $J = 20$ [16].

Experimental spectroscopic measurements of H_2CS will be discussed in detail in Section 3 and we mention only a few studies here. One of the few high-resolution studies of H_2CS was conducted in the $10\,\mu m$ region [17] studying the three lowest fundamental bands, namely the C–S stretching mode ν_3, the out-of-plane CH_2 wagging mode ν_4, and the in-plane CH_2 rocking mode ν_6. Recorded using a Fourier-transform spectrometer at a resolution of $0.005\,cm^{-1}$, the study highlighted the massive Coriolis interaction that occurs between the ν_4 and ν_6 modes, whose band centres are separated by less than $1\,cm^{-1}$. Pure rotational spectra of H_2CS [18] and seven of its isotopologues [19] have been measured, yielding highly accurate datasets that are particularly valuable for astronomical observations in intersteller environments. Other laboratory measurements have tended to be at low to medium-resolution but still provide important transition data, for example, covering the ν_1, ν_5 and $2\nu_2$ bands located around $3000\,cm^{-1}$ [20].

* Corresponding author.
E-mail addresses: thomas.mellor.14@ucl.ac.uk (T.M. Mellor), s.yurchenko@ucl.ac.uk (S.N. Yurchenko).
[1] All authors contributed equaly.

https://doi.org/10.1016/j.jms.2022.111732
Received 1 October 2022; Received in revised form 28 November 2022; Accepted 5 December 2022
Available online 9 December 2022

Table 1
Extract from the MARVEL transition file. The MARVEL frequency wavenumber $\tilde{\nu}$ and uncertainties are in cm^{-1}. There are two uncertainty columns to allow the input uncertainty to be updated while retaining the original uncertainty of the source.

$\tilde{\nu}$	unc. (cm^{-1})	unc. (cm^{-1})	Quantum 'numbers' of upper states									Quantum 'numbers' of lower states									Source
			J'	K'_a	K'_c	n'_1	n'_2	n'_3	n'_4	n'_5	n'_6	J''	K''_a	K''_c	n''_1	n''_2	n''_3	n''_4	n''_5	n''_6	
8.01661895	0.00000167	0.00000167	7	4	4	0	0	0	0	0	0	6	4	3	0	0	0	0	0	0	08MaMeWiDe.35

In this work we perform an extensive spectroscopic literature analysis of H_2CS and extract all meaningful transitions into a consistent, labelled dataset with measurement uncertainties. This dataset is processed using the MARVEL (Measured Active Rotational-Vibrational Energy Levels) algorithm [21–24] to produce an extensive list of ro-vibrational energy levels of H_2CS in its ground electronic state. Such MARVEL datasets are finding widespread use in molecular line list production for the ExoMol database [25] with two major applications. Firstly, the underlying molecular PES can be empirically-refined to the dataset to improve the accuracy of the calculated ro-vibrational energy levels, resulting in orders-of-magnitude improvements in the accuracy of the predicted transition wavenumbers. Secondly, once a line list has been computed, the calculated energy levels can be replaced by the empirically-derived MARVEL values, for example, as was recently done for AlO [26]. A recent MARVEL study on formaldehyde (H_2CO) [27] identified 16 403 validated, unique transitions which provided 5029 empirical energy levels. Using the levels to update the AYTY ExoMol line list [28] resulted in 367 779 transitions whose wavenumbers are empirically determined; approximately half these transitions are strong enough to be included in the HITRAN database [29] and these data are currently being used to update HITRAN. MARVEL energies therefore can be used to tailor a line list in certain spectroscopic regions towards high-resolution applications, making them applicable, for example, to study exoplanets using high resolution Doppler shift spectroscopy [30, 31].

2. MARVEL procedure

2.1. The approach and input structure

Based on the theory of spectroscopic networks [23,32–34], MARVEL takes a user-constructed dataset of assigned spectroscopic transitions and converts them into a consistent set of labelled energy levels with the measurement uncertainties propagated from the input transitions to the output energies. MARVEL can be accessed via the online app at http://kkrk.chem.elte.hu/marvelonline. From a user-perspective, the MARVEL input dataset of transitions has the general structure

$\tilde{\nu}$ in. unc. up. unc. QN′ QN″ source.i

where $\tilde{\nu}$ is the transition wavenumber (cm^{-1}), in. unc is the initial measurement uncertainty (cm^{-1}), up. unc is the updated uncertainty (cm^{-1}) which may differ from the initial uncertainty, QN′ and QN″ are the quantum numbers of the upper and lower states involved in the transition, respectively, and source.i is the literature source tag concatenated with a counting number i of the datum from this source. source.i is a unique ID of the transition in the dataset and is required by MARVEL. The source tag, for example 72BeKlKiJo, is based on the notation employed by the IUPAC task group on water [35,36] and is generally speaking formed from the year published and the first two letters of, up to, the initial four authors' surnames. An extract of the MARVEL input file of H_2CS containing the labelled transitions is shown in Table 1.

2.2. H_2CS quantum numbers

H_2CS is a semi-rigid, asymmetric top molecule that can be classified according to the C_{2v}(M) molecular symmetry group with the irreducible representations $\{A_1, A_2, B_1, B_2\}$ [37]. Transitions follow the symmetry selection rules $A_1 \leftrightarrow A_2$ and $B_1 \leftrightarrow B_2$; and the standard rotational selection rules, $J' - J'' = 0, \pm 1$, $J' + J'' \neq 0$; where $'$ and $''$ denote the upper and lower state, respectively.

Table 2
Symmetry species of J_{K_a,K_c} levels of H_2CS in the C_{2v}(M) group [37].

K_a	K_c	Γ_{rot}
even	even	A_1
even	odd	A_2
odd	even	B_2
odd	odd	B_1

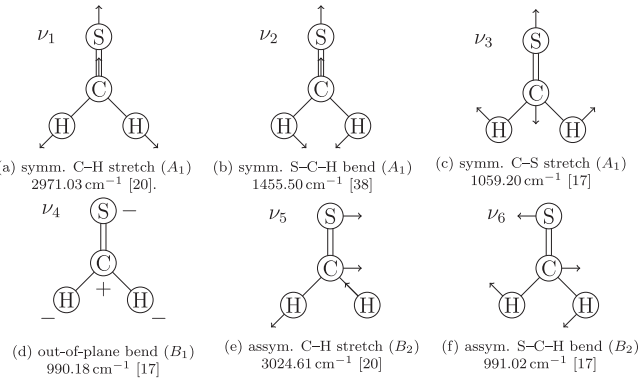

Fig. 1. Vibrational modes and measured band centres of H_2CS.

Nine quantum numbers were required to uniquely label a rotation-vibration energy level of H_2CS in the ground electronic state: the six vibrational normal mode quantum numbers n_1–n_6 associated with the six normal modes ν_1–ν_6 detailed in Fig. 1, and the three standard rigid-rotor quantum numbers J, K_a, K_c. Here, J is the total angular momentum quantum number, K_a and K_c are the oblate and prolate quantum numbers, respectively. These are restricted by the convention $J = K_a + K_c$ or $J = K_a + K_c + 1$ (the latter only when $K_a \neq 0$ and $K_c \neq 0$), depending on the symmetry of rotational state, see Table 2. This gives $2J + 1$ states for a given J. Only J and the total irreducible representation are rigorous quantum labels, while n_1–n_6, K_a and K_c are approximate quantum numbers.

Table 2 shows the relationship between the rotational quantum numbers and overall rotational symmetry. This needs to be combined with the symmetry of the vibrational modes given above to give the total symmetry of a given state.

The chosen set of quantum numbers has to be consistent across the whole dataset and care must be taken when extracting data from literature sources as different labelling conventions are occasionally encountered.

3. Experimental data sources

Spectroscopic data was extracted from 11 published sources and these are summarised in Table 3. This table gives the energy and J range of each source, the bands covered, the number of available transitions (A), the number of validated transitions (V) by the MARVEL procedure, and, from those validated transitions, the mean and maximum uncertainty obtained from the uncertainties quoted in each study. Three sources provided their original data in digital format, while the other literature sources were processed using *ABBYY FineReader*. The

Table 3
Experimental literature sources of H_2CS spectra and their coverage. For the MARVEL analysis, V is the number of verified transitions and A is the number of available transitions. The mean and maximum uncertainties of each dataset reflects only the verified transitions.

Tag	Energy range (cm^{-1})	Band	J range	V/A	Unc. Mean/Max (cm^{-1})
70JoPo [38]	0.209 – 0.349	ν_0	3 – 4	2/2	$3.34\times10^{-7}/3.34\times10^{-7}$
71JoOl [20]	2843 – 3129	ν_1, $2\nu_2$, ν_5	0 – 30, 1 – 30, 2 – 24	1110/1478	$7.559\times10^{-3}/2.000\times10^{-2}$
72BeKlKiJo [39]	0.105 – 8.141	ν_0	0 – 27	56/56	$1.167\times10^{-4}/2.715\times10^{-4}$
77FaKrMu [40]	0.0349	ν_0	0 – 1	1/1	$2.23\times10^{-9}/2.23\times10^{-9}$
80BeDu [41]	924.9 – 1059	ν_3, ν_4, ν_6	1 – 6, 3 – 9, 3 – 9	63/82	$2.000\times10^{-3}/2.000\times10^{-3}$
81TuHaMi [42]	818.8 – 1221	ν_4, ν_6	0 – 22, 2 – 23	102/386	$3.839\times10^{-3}/2.800\times10^{-2}$
93McBr [43]	31.46 – 1499	ν_0, ν_2	21 – 54, 1 – 37	922/935	$3.256\times10^{-2}/5.000\times10^{-2}$
94ClHuAdMe [44]	2.222 – 402.1	ν_0	0 – 36	302/355	$4.000\times10^{-4}/4.000\times10^{-4}$
08MaMeWiDe [18]	4.161 – 12.40	ν_0	4 – 41	113/113	$1.980\times10^{-6}/3.340\times10^{-6}$
19MuMaTh [19]	4.161 – 46.23	ν_0	4 – 42	317/317	$1.020\times10^{-6}/3.336\times10^{-6}$
08FlLaPeKi [17]	690.7 – 1338	ν_3, ν_4, ν_6	0 – 50, 0 – 50, 1 – 51	8649/8655	$4.748\times10^{-4}/1.000\times10^{-3}$

number of available transitions for a given source does not include transitions taken from prior sources.

There were two primary reasons for the exclusion of a transition. The first is when its provenance was not clear so the line could not be verified to be purely experimental. The second is when the difference between the energy of a state determined by the MARVEL procedure compared to the energy as predicted by a transition was greater than the uncertainty of the transition. Typically, these states were well supported by several other transitions (from another source) with the outlier transition biasing the MARVEL energy of the state towards the transition-predicted energy even if the transition uncertainty was increased. Thus, the removal of the transition improved the final MARVEL energy. A negative sign is added to any transition wavenumber to remove it from the MARVEL procedure.

A number of changes were made to the extracted transition data. The energies of states with K_a close to J may depend only very weakly on K_c and often give rise to two very-closely-spaced transitions, a phenomenon known as K-doubling. In sources where the prolate (K_c) quantum numbers were missing, degenerate transitions with both possible values were added into the input transitions file which respected the symmetry rule. The number of available transitions in Table 3 reflects this change.

Due to the close band centres of ν_4 and ν_6, the vibrational assignment of the upper states is somewhat ambiguous. Consequently, the ν_4/ν_6 assignments across literature sources were not all compatible with each other. For many transitions, their upper vibrational states had to be relabelled to ensure consistency in the input transitions file. The basis and method of the relabelling is explained in Section 3.2, with the changes made to the individual sources detailed below. First we give details of the sources we included in our MARVEL analysis.

70JoPo [38]: A ground vibrational study whose data was included in 19MuMaTh.

71JoPoKi [45]: A ground vibrational study whose data was included in 72BeKlKiJo.

71JoOl [20]: An infrared study with the ν_1, ν_5, and $2\nu_2$ bands. The original assignment for the latter was $2\nu_6$ but this was incorrect and has since been updated. The transitions from this source were challenging to scan due to the print quality and were not always unambiguous. The transitions were also of relatively low resolution as illustrated in Fig. 2. This paper had the largest number of non-validated transitions. These were the asterisk-marked transitions in their publication, which, in certain cases, were unobserved but expected transitions, however the precise transitions where this applied was not specified. Thus, all had to be removed from the validated set. These were labelled with a "_a" after the source number but before the label number. In total, 368 transitions were removed for this reason or because the energy they predicted deviated from that predicted by MARVEL beyond their uncertainty.

72BeKlKi [39]: Microwave study up to $J = 27$. No difficulties in validating the transitions.

77FaKrMu [40]: One measured line from this study was included in the 19MuMaTh dataset.

80BeDu [41]: Infrared study involving the ν_3, ν_4, and ν_6 bands. 19 transitions were removed as the energy they predicted deviated from that predicted by MARVEL beyond their uncertainty.

08FlLaPeKi [17]: An infrared study of the ν_3, ν_4, and ν_6 bands. The authors of this study were contacted and they provided a more complete set of data which was used in the MARVEL analysis. Several quantum numbers were adjusted. 18 lines had the K'_a quantum number increased by 2 with the corresponding K'_c quantum number decreased by 2 to maintain the symmetry and $K'_a + K'_c$ requirement. 2919 lines had their K'_c value adjusted by 1 or −1 so that the symmetry selection rule was satisfied. Finally, 1625 lines had their ν_4 and ν_6 assignment swapped (discussed in Section 3.2). 6 transitions were removed as their optimal uncertainty was too high.

81TuHaMi [42]: Infrared study involving the ν_3, ν_4, and ν_6 bands. Some listed transitions were taken from 80BeDu so we ignored these and used the original data source. These were labelled with a "_o" after the source name but before the label number. 8 transitions had their ν_4 and ν_6 assignment swapped. 10 transitions had their K'_c values changed by 1, three had their K'_c values changed by 2, and one had its K'_c value changed by 3. One transition had its K'_a value changed by 1 and four had their K'_a values changed by 2. Eight transitions had their K''_c values changed by 1. One transition had its K''_a values changed by 1 and one had its K''_a value changed by 2. 284 transitions were removed as the energy they predicted deviated from that predicted by MARVEL beyond their uncertainty.

93McBr [43]: The authors of this study were contacted and they provided us with the transitions from the ν_2 band. It is the only source containing the ν_2 band; the transitions are relatively low resolution, as illustrated in Fig. 2 where the highest circle for 93McBr corresponds to the ν_2 transitions. No subsequent high resolution studies of this band have been undertaken. Microwave transitions from this source are contained in 19MuMaTh and 08MaMeWiDe.

94ClHuAdMe [44]: An electronic study of the $\tilde{A}$–$\tilde{X}$ transition of thioformaldehyde. The ground state combination differences reported in 19MuMaTh and taken from this study were used in the MARVEL dataset. 53 transitions were removed as the energy they predicted deviated from that predicted by MARVEL beyond their uncertainty.

08MaMeWiDe [18]: A microwave study which included transition data from multiple sources including 94ClHuAdMe, 71JoPoKi, 80BeDu, 72BeKlKiJo, 93McBr as well as CDMS [46] data and FASSST [47] data. Transitions in the MARVEL input file from 93McBr numbered 113 and above are from this source.

19MuMaTh [19]: A microwave study which incorporated data from multiple sources including 77FaKrMu, 70PoJo, 71JoPoKi, 72BeKlKiJo,

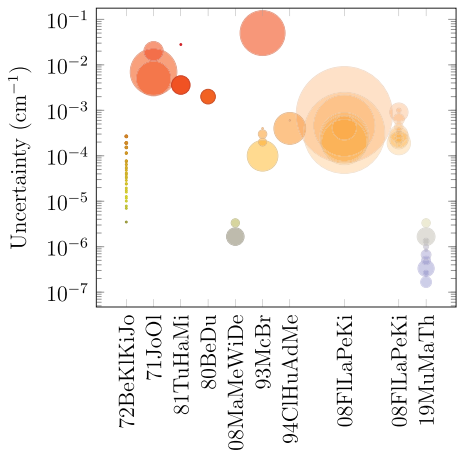

Fig. 2. Uncertainties in the measured data (vertical axis, log scale) from each literature source (horizontal axis). Each circle corresponds to a given uncertainty. The vertical coordinate of the centre of the circle is the uncertainty, and the area of the circle is proportional to the number of transitions with that uncertainty. The smallest and largest circles correspond to 1 and 2729 transitions, respectively.

94ClHuAdMe, and 93McBr. It also contained CDMS and FASSST data. Transitions from 93McBr numbered 1–112 are from this source.

There is an overlap in data coverage from the sources 08FlLaPeKi, 80BeDu, and 81TuHaMi as, collectively, they contained transitions involving the ν_3, ν_4, and ν_6 bands. Fig. 2 illustrates the uncertainties of the data by source. The uncertainties of 08BeDu and 81TuHaMi were consistently higher than the ones from 08FlLaPeKi. 08FlLaPeKi's dataset was also significantly larger and, consequently, each state was well represented by several transitions. Due to the lower uncertainties, transitions to a given upper state were much more internally consistent. Because of these factors, 08FlLaPeKi was favoured over the other two sources. In total, 19 transitions from 80BeDu and 284 transitions from 81TuHaMi were removed because they were not in agreement with the other data.

3.1. Artificial transitions

The ro-vibrational states of H_2CS are either ortho or para due to the nuclear spins of the hydrogen atoms. As a result, the MARVEL analysis produces two separate networks of energy levels, an ortho-network and a para-network, which are disconnected. To ensure the relative energies of the networks are correct and correspond to the ro-vibrational ground state of the molecule, it is necessary to link the ortho-network and para-network through an artificial transition. This was done using the pseudo-experimental transition wavenumbers reconstructed with the PGOPHER program [48] where the spectroscopic constants were taken from 08FlLaPeKi. An artificial microwave transition $1_{11} \leftarrow 0_{00}$ (states labelled as $J_{K_aK_c}$) with a value of 10.281 825 81(33) cm^{-1} was added to the input MARVEL transition file to link the networks.

3.2. Relabelling the ν_4 band and ν_6 band transition data

The out-of-plane bending mode ν_4 and the asymmetric S–C–H bending mode ν_6 have very close band centres and interact through a massive A-type Coriolis resonance [17]. As has been mentioned, the consequence of this is that there is an ambiguity in the vibrational (i.e. approximate) assignment of these bands in different literature sources. To ensure compatibility across all literature sources, a number of transitions involving these vibrational bands had to be relabelled. It was decided that for ambiguously assigned transitions, the vibrational labels given by the variational nuclear motion code TROVE [49] would be used. There were two reasons for this. First, the TROVE dataset contained a complete set of computed energy levels of H_2CS, which included the experimentally verified states from our MARVEL set. Since the TROVE dataset is internally consistent, it was logical to use it to ensure consistency across the experimental data sources as well. If subsequent experiments with these modes become available, the TROVE dataset may be once again utilised in this manner. The second reason is that calculations form the basis of a new comprehensive MARVELised hot line list of thioformaldehyde, the details of which will be reported elsewhere [50]. If the TROVE quantum numbers were adjusted to match the assignment of a literature source, further reassignments of TROVE states would be necessary – to ensure internal consistency across the whole TROVE dataset – without an external source as a basis for it. For details of the mapping of TROVE quantum numbers to the experimental quantum numbers, see [50].

For the MARVEL input file, the relabelling process involved swapping the upper state v_4' and v_6' quantum numbers in transitions from the literature sources 08FlLaPeKi and 81TuHaMi (see Table 3). Also, the upper state K_c' value was changed by 1 or −1 to maintain the symmetry selection rule of the transition while also ensuring that the convention $J' = K_a' + K_c'$ or $J' = K_a' + K_c' + 1$ was satisfied. The rotational quantum numbers K_a were kept unchanged. To generate the lower state energies, the computer program PGOPHER [48] was used with the spectroscopic constants given in 08FlLaPeKi. Since the lower states were purely rotational, there was no ambiguity in their assignment.

4. Results

4.1. MARVEL analysis

The MARVEL analysis was performed using the compiled MARVEL version 3 with the Cholesky (analytic) method. An extract from the output MARVEL energy level file is shown in Table 4. In total, 11 638 non-unique transitions out of 12 380 transitions up to $J = 54$ were processed, resulting in 4254 ro-vibrational energy levels up to 3729.07 cm^{-1}. Using the new ExoMol H_2CS line list [50] shows the number of transitions between MARVEL states stronger than 1×10^{-30} cm/molecule (the HITRAN threshold) is 74 425.

Fig. 3 shows the energy level coverage of the MARVEL ro-vibrational states as a function of J for the different vibrational bands. Each vibrational band is illustrated by colour but within each band the different K_a and K_c states have the same colour. Fig. 4 shows the ν_4 and ν_6 in more detail as reduced energies, Energy $- 0.572J(J+1) - 9.18K_a^2$ (cm^{-1}), are plotted as function of J. $BJ(J+1) + (A-B)K_a^2$ is the approximate rotational dependence of the ro-vibrational energy for an prolate symmetric top, where A and B are rotational constants [37]. The values chosen for the plots are close to, but deviate from, these values. Each vibrational band is separately illustrated but within each band the different K_a and K_c states have the same colour. For moderate to high K_a values, TROVE almost consistently labels states of higher energy as ν_6 states which provides further justification for basing the experimental MARVEL assignment on the TROVE assignment. This is not the case for low K_a values; we further examine these states below.

Table 5 shows the lowest energy state of each fundamental band as determined by MARVEL, as well as the predicted band centre, which was obtained by subtracting the energy of the pure rotational state from the ro-vibrational state. These values can be compared to the experimentally measured band centres quoted in Fig. 1, and we see that for the ν_3, ν_4 and ν_6 modes the MARVEL band centres are the same to within two decimal places. For the other fundamentals, the MARVEL band origins deviate from the measured band centres at the second decimal place. We can assess this deviation by comparing the minimum (or maximum) possible value of the experimental band centre (those quoted in Fig. 1) and the predicted MARVEL band centre. For example, the minimum possible value for ν_1 is 2971.025 cm^{-1} and the MARVEL band centre is 2971.018 16 cm^{-1}. Thus, the deviation is 0.006 84 cm^{-1}. For the bands ν_2 and ν_5, the MARVEL energies are different by 0.0273 cm^{-1}

Table 4
Extract from the MARVEL energy file. The quantum numbers/labels are described in the text and are followed by the MARVEL energy term value (cm^{-1}), the uncertainty of the state (cm^{-1}), and the number of transitions supporting the state in question.

Quantum 'numbers'									$\tilde{E}$	Unc.	No. of
J	K_a	K_c	n_1	n_2	n_3	n_4	n_5	n_6	cm^{-1}	cm^{-1}	trans.
5	2	3	0	0	0	0	0	0	53.792652349	0.000316979	27
9	1	9	0	0	0	0	0	0	59.916981444	0.000135763	28
6	2	5	0	0	0	0	0	0	60.662392583	0.000316979	28
6	2	4	0	0	0	0	0	0	60.669363102	0.000316975	25
9	1	8	0	0	0	0	0	0	61.486995429	0.000135763	28

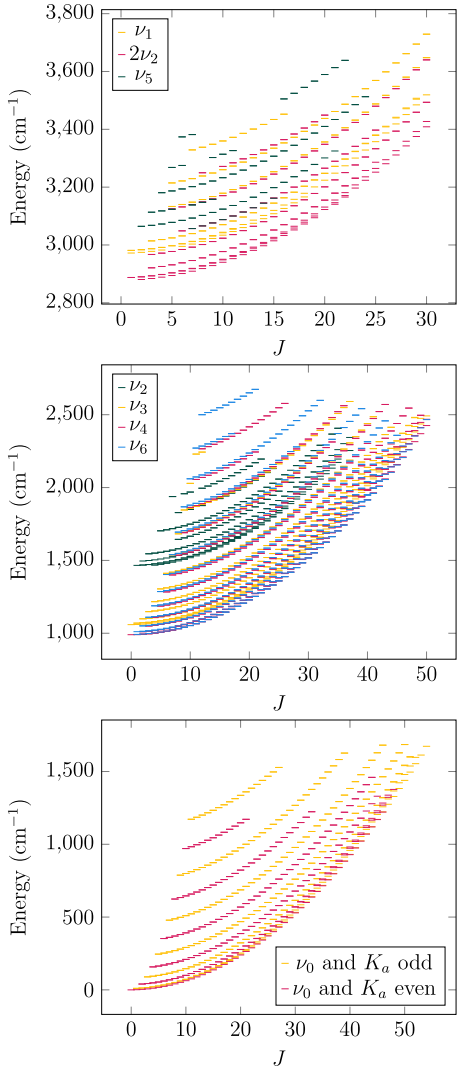

Fig. 3. The MARVEL energy term values of each state as a function of the angular momentum quantum number, J. Multiple states from the same band with the same J have different K_a and K_c numbers (not labelled). The ground vibrational state (ν_0) energies are separated by the ortho (K_a odd) or para (K_a even) splitting.

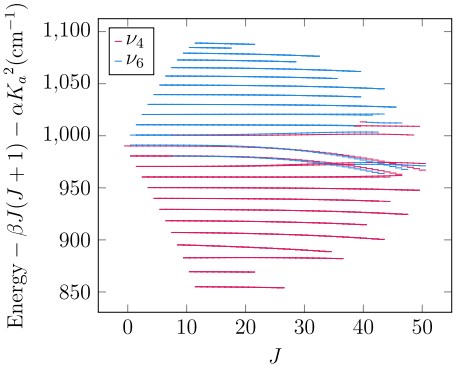

Fig. 4. Reduced MARVEL energies of the ν_4 and ν_6 as Energy $-\beta J(J+1)-\alpha K_a{}^2$ ($\alpha = 9.18\,cm^{-1}$ and $\beta = 0.572\,cm^{-1}$) plotted as a function of the angular momentum quantum number, J.

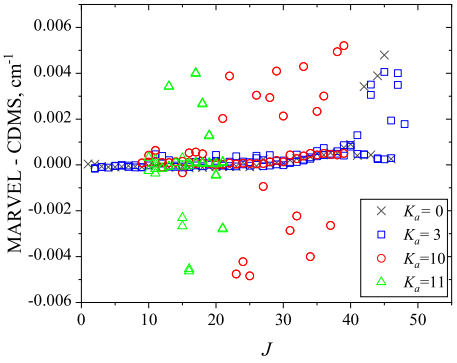

Fig. 5. Difference between vibrational ground vibrational state energies (ν_0) from MARVEL and CDMS (cm^{-1}) as a function of J for states with selected oblate quantum number values of K_a.

and $0.0006\,cm^{-1}$, respectively. This is not wholly unexpected, however, as the associated experiments were of lower accuracy. Consequently, the MARVEL uncertainties on the lowest energy states for these bands are $0.007\,cm^{-1}$, $0.05\,cm^{-1}$, and $0.007\,cm^{-1}$, respectively.

Fig. 5 shows the difference between the available CDMS [51] and MARVEL ν_0 (ground vibrational) energies for selected values of K_a. The CDMS energy terms values were generated by taking the union of the lower state energies and the lower state energy plus the transition wavenumber. The sources were essentially the same as the ground vibrational sources used for the MARVEL analysis. The lower values of K_a have lower discrepancies ($< 0.001\ cm^{-1}$) which grow with J and K_a. The average uncertainty of the MARVEL ground vibrational energies is $7.75 \times 10^{-4}\,cm^{-1}$. Thus, the agreement is good, and the lack of any significant outlier implies that no state has an incorrect energy or assignment.

Fig. 6(a) shows examples of the original 08FlLaPeKi assignment for the ν_4 and ν_6 for both $K_a = 1$ and $K_a = 2$ where we have plotted the 08FlLaPeKi energy minus $BJ(J+1)$, with B being the rotational constant – a measure of the approximate J energy dependence. This reduces the energy range and thus increases the readability of the plot. There is an apparent misassignment of the ν_4 and $K_a = 2$ energies in the region $20 < J < 30$. The TROVE assignment, shown in Fig. 6(b), partially rectifies this issue.

However, there are still graphically-incorrect vibrational assignments for ν_4, $K_a = 2$ and ν_6, $K_a = 2$. Swapping the vibrational labels for these states for $J > 37$ resulted in the relabelling shown in Fig. 7. For the ν_6 and $K_a = 2$ state, one notes the peculiar behaviour of the energy difference between the two K_a states. This is due to a resonance

Table 5
MARVEL energies of states from each band with the associated quantum numbers and symmetry. The MARVEL uncertainty and the number of transitions supported a state (No. trans.) are also quoted. Above dividing line: The MARVEL energies from the lowest lying state from each band as well as the band centre which is obtained by subtracting the MARVEL energy of the purely rotational state from the ro-vibrational energy. Below dividing line: The subsequent states from each band.

$(J_{K_aK_c}n_1n_2n_3n_4n_5n_6)$	Irrep	MARVEL energy (cm^{-1})	Uncertainty (cm^{-1})	No. trans.	Band centre (cm^{-1})
$(0_{00}000000)$	A_1	0.000 00	0.000 00	8	0.000 00
$(1_{01}100000)$	B_1	2972.164 00	0.007 00	1	2971.018 16
$(1_{11}010000)$	A_2	1465.859 13	0.050 00	1	1455.577 31
$(2_{02}020000)$	A_1	2880.555 12	0.007 00	2	2877.117 72
$(0_{00}001000)$	A_1	1059.204 76	0.000 46	1	1059.204 76
$(0_{00}000100)$	B_1	990.182 14	0.000 47	2	990.182 14
$(7_{07}000010)$	A_2	3056.673 37	0.007 00	1	3024.604 40
$(1_{01}000001)$	A_2	992.164 06	0.000 80	2	991.018 22
$(1_{01}000000)$	A_2	1.145 84	0.000 04	10	
$(2_{02}000000)$	A_1	3.437 39	0.000 09	15	
$(3_{03}000000)$	A_2	6.874 40	0.000 14	16	
$(2_{02}100000)$	A_1	2974.459 84	0.005 00	1	
$(3_{03}100000)$	B_1	2977.888 23	0.005 00	2	
$(1_{11}100000)$	B_1	2981.234 12	0.005 00	2	
$(4_{04}010000)$	A_2	1466.957 07	0.050 00	1	
$(2_{12}010000)$	B_1	1468.113 36	0.050 00	2	
$(2_{11}010000)$	B_2	1468.227 40	0.050 00	2	
$(3_{03}020000)$	A_2	2884.022 50	0.007 00	2	
$(1_{11}020000)$	B_1	2887.486 73	0.007 00	1	
$(1_{10}020000)$	B_2	2887.524 03	0.007 00	2	
$(1_{01}001000)$	A_2	1060.345 03	0.000 91	2	
$(2_{02}001000)$	A_1	1062.625 43	0.000 46	2	
$(3_{03}001000)$	A_2	1066.045 82	0.000 47	2	
$(1_{11}000100)$	A_1	990.884 14	0.002 00	1	
$(1_{10}000100)$	A_2	990.885 04	0.000 80	3	
$(1_{01}000100)$	B_2	991.325 47	0.000 34	3	
$(2_{20}000010)$	B_2	3064.413 53	0.007 01	1	
$(2_{21}000010)$	B_1	3064.413 53	0.007 01	1	
$(8_{08}000010)$	B_2	3065.845 98	0.007 00	1	
$(2_{02}000001)$	B_2	994.451 57	0.000 81	3	
$(3_{03}000001)$	B_1	997.882 37	0.000 81	3	
$(4_{04}000001)$	B_2	1002.455 90	0.000 82	3	

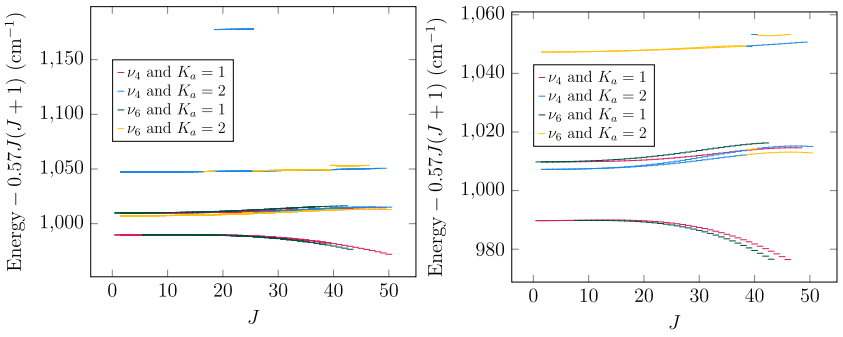

(a) 08FlLaPeKi assignment.

(b) TROVE assignment.

Fig. 6. Reduced MARVEL energy term values (Energy − $0.57J(J+1)$, cm^{-1}) of the $K_a = 1$ and $K_a = 2$ states for the ν_4 and ν_6 bands as a function of the angular momentum quantum number, J.

interaction with the nearby ν_3, $K_a = 1$ states, also shown in Fig. 7. The lower lying ν_3, $K_a = 1$ states have symmetries which alternate between B_1 and B_2 in step with the upper lying ν_6, $K_a = 2$ states. The supplementary material contains the MARVEL input file which includes the graphically relabelled states of Fig. 7.

A further seemingly problematic set of assignments are for the $K_a = 0$ and $K_a = 1$ states of the ν_4 and ν_6 bands, the ν_4 band being shown in Fig. 8. In these cases, rather than the two near-degenerate states being those with the same K_a, one is assigned as the $K_a = 0$ state and the other the $K_a = 1$ state. The other $K_a = 1$ state is assigned to the energy further away from the near-degenerate states. This is because of the strong interaction, and hence mixing, between these two levels. These are the only states that cannot be vibrationally reassigned as it would involve changing ortho states to para states: the K_a value from odd to even (or vice versa) which changes the symmetry from A type to B type (or vice versa) (see Table 2).

The uncertainties for each state by band are shown in Fig. 9. One notes the expected behaviour for the vibrational ground state (ν_0), ν_3, ν_4, and ν_6 bands. The input data for these bands was primarily from 08MaMeWiDe, 19MuMaTh, and 08FlLaPeKi, which are of higher quality than the sources used for the other bands. The energies for the other bands are sourced exclusively from 93McBr and 71JoOl. Fig. 9

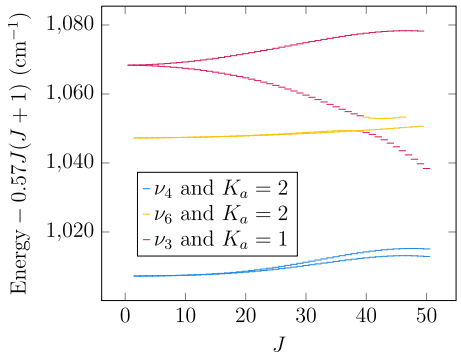

Fig. 7. A plot of the Energy $-0.57J(J+1)$ of the $K_a = 1$ and $K_a = 2$ states for the ν_4 and ν_6 bands as a function of the angular momentum quantum number, J. This is after the $J > 37$ states of ν_4 and $K_a = 2$ and ν_6 and $K_a = 2$ were swapped. The states ν_3 and $K_a = 1$ are also shown.

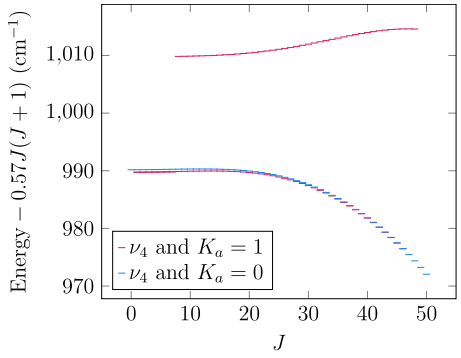

Fig. 8. Reduced energy term values (Energy $-0.57J(J+1)$) of the $K_a = 1$ and $K_a = 0$ states for the ν_4 band as a function of the angular momentum quantum number, J. These were sourced from the energy levels file of the MARVEL output after the transitions were relabelled using TROVE.

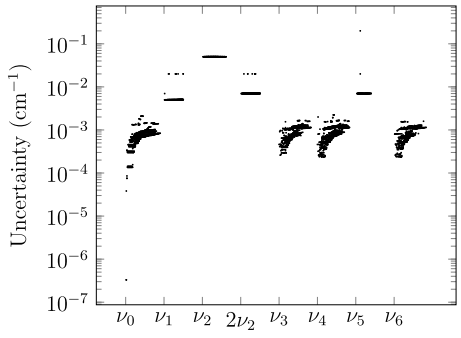

Fig. 9. Uncertainty of the MARVEL energies levels (vertical axis, log scale) split by band (horizontal axis). The uncertainties are plotted as a function of J. The left-most uncertainty corresponds to $J = 0$ states while the crossover point to the next band corresponds to $J = 60$. Multiple states from the same band with the same J number have different K_a and K_c numbers.

shows that their uncertainty is flat rather than growing with J. This is a result of both large input uncertainties, as shown on Fig. 2, with a mean of 7.56×10^{-3} cm^{-1} and 2.00×10^{-3} cm^{-1} for 71JoOl and 93McBr, respectively, and for uniform uncertainties for all transitions within a band.

Finally, Fig. 10 shows the energy of each state minus its band centre split by band. The size of each point is proportional to the number of transitions that support that state. The ν_0, ν_3, ν_4, and ν_6 states are measured up to a higher rotational excitation with states up to $J = 51$.

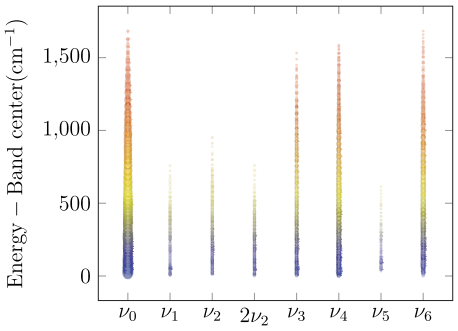

Fig. 10. The energy of each state minus the band centre of each state (the vertical axis) split by band (the horizontal axis) in cm^{-1}. Each circle corresponds to a given state. The vertical coordinate of the centre of the circle is the energy of the state minus the band centre, and the area of the circle is proportional to the number of transitions that supports that state. The maximum number of supporting transitions is 35.

The maximum rotational excitation has a range of $J = 24$ to $J = 37$ for the other bands.

The number of transitions characterising each state varies between bands. The largest number is for the ν_0 band where the maximum for a single state is 35 transitions. States in the ν_4 and ν_6 bands are also well characterised, although not as well as ν_0, with a maximum of 9 transitions to a single state. The characterisation of the remaining states is less good, with several higher rotationally excited states in ν_1, ν_2, $2\nu_2$, ν_6, and, to a lesser extent, ν_3 being only supported by a single transition. ν_3's maximum is 6 while the rest have a maximum of 3. The MARVEL output energies for states only characterised by a single transition are less trustworthy and depend largely on the accuracy of the stated uncertainty of the experiment; transitions to these states cannot be compared to ensure consistency and accuracy.

5. Conclusions

A comprehensive analysis of the published spectroscopic literature of the main isotopologue of thioformaldehyde ($^1H_2{}^{12}C^{32}S$) has been performed. All meaningful transitions from 11 literature sources have been extracted and verified, resulting in 11 638 validated transitions using the MARVEL algorithm. The data covers the ground, ν_1, ν_2, ν_3, ν_4, ν_5, ν_6, and $2\nu_2$ vibrational bands and produced 4254 ro-vibrational energy levels up to $J = 54$ below 3729 cm^{-1}. Both the MARVEL input file containing the quantum number labelled transitions with measurement uncertainties and the MARVEL output file containing the quantum number labelled ro-vibrational energy levels with uncertainties are provided in the supplementary material.

Comparison of the MARVEL input file with variational line list calculations revealed numerous incompatible vibrational assignments in the experimental transition data, largely concerning the ν_4 and ν_6 modes which are very close in energy and interact through a strong Coriolis resonance. The ability to relabel the transitions in a consistent manner that respected molecular symmetry and quantum number selection rules highlighted the significance of rigorous theoretical calculations to confirm experimental findings. This relationship goes both ways as the output MARVEL energy levels are extremely valuable in improving theoretical line list calculations, for the reasons discussed earlier. Notably, the H_2CS MARVEL energies presented in this work have been utilised in the production of a new line list of thioformaldehyde applicable to high temperatures (up to 2000 K), named MOTY, that will be reported elsewhere [50]. The MOTY line list contains over 43 billion transitions and will be available from the ExoMol database [25]. As an important astrophysical molecule, we expect the MOTY line list and the MARVEL H_2CS datasets presented here to be useful in various spectroscopic and radiative applications.

Declaration of competing interest

The authors declare that they have no known competing financial interests or personal relationships that could have appeared to influence the work reported in this paper.

Data availability

The data are provided as part of the supplementary material.

Acknowledgements

We dedicate this article to the memory of Colin Western and acknowledge his great help that he was always ready to provide. We thank T. Furtenbacher for providing access to his MARVEL codes. We also thank J.-M. Flaud for providing us with a more complete set of transition data which was the basis for the 08FlLaPeKi and we thank D. McNaughton for providing the set of transitions for the ν_2 band as reported in 93McBr.

This work was supported by the STFC Projects No. ST/M001334/1 and ST/R000476/1. The authors acknowledge the use of the UCL Legion High Performance Computing Facility (Legion@UCL) and associated support services in the completion of this work, along with the Cambridge Service for Data Driven Discovery (CSD3), part of which is operated by the University of Cambridge Research Computing on behalf of the STFC DiRAC HPC Facility (www.dirac.ac.uk). The DiRAC component of CSD3 was funded by BEIS capital funding via STFC capital grants ST/P002307/1 and ST/R002452/1 and STFC operations grant ST/R00689X/1. DiRAC is part of the National e-Infrastructure. This work was also supported by the European Research Council (ERC) under the European Union's Horizon 2020 research and innovation programme through Advance Grant number 883830.

Appendix A. Supplementary data

Supplementary material related to this article can be found online at https://doi.org/10.1016/j.jms.2022.111732.

References

[1] M.W. Sinclair, N. Fourikis, J.C. Ribes, B.J. Robinson, R.D. Brown, P.D. Godfrey, Detection of interstellar thioformaldehyde, Aust. J. Phys. 26 (1973) 85, http://dx.doi.org/10.1071/ph730085.

[2] S. Martín, J. Martín-Pintado, R. Mauersberger, C. Henkel, S. García-Burillo, Sulfur chemistry and isotopic ratios in the starburst galaxy NGC 253, Astrophys. J. 620 (2005) 210–216, http://dx.doi.org/10.1086/426888.

[3] A. Heikkilä, L.E.B. Johansson, H. Olofsson, Molecular abundance variations in the magellanic clouds, Astron. Astrophys. 344 (1999) 817–847.

[4] S. Muller, A. Beelen, M. Guélin, S. Aalto, J.H. Black, F. Combes, S.J. Curran, P. Theule, S.N. Longmore, Molecules at z=0.89, Astron. Astrophys. 535 (2011) A103, http://dx.doi.org/10.1051/0004-6361/201117096.

[5] G. Esplugues, A. Fuente, D. Navarro-Almaida, M. Rodríguez-Baras, L. Majumdar, P. Caselli, V. Wakelam, E. Roueff, R. Bachiller, S. Spezzano, P. Rivière-Marichalar, R. Martín-Doménech, G.M. Muñoz Caro, Gas phase Elemental abundances in Molecular cloudS (GEMS), Astron. Astrophys. 662 (2022) A52, http://dx.doi.org/10.1051/0004-6361/202142936.

[6] L.M. Woodney, M.F. A'Hearn, J. McMullin, N. Samarasinha, Sulfur chemistry at millimeter wavelengths in C/Hale-Bopp, Earth Moon Planets 78 (1997) 69–70, http://dx.doi.org/10.1023/A:1006275412491.

[7] S. Doddipatla, C. He, R.I. Kaiser, Y. Luo, R. Sun, G.R. Galimova, A.M. Mebel, T.J. Millar, A chemical dynamics study on the gas phase formation of thioformaldehyde (H_2CS) and its thiohydroxycarbene isomer (HCSH), Proc. Natl. Acad. Sci. 117 (2020) 22712–22719, http://dx.doi.org/10.1073/pnas.2004881117.

[8] C. He, S.M. Hörst, N.K. Lewis, X. Yu, J.I. Moses, P. McGuiggan, M.S. Marley, E.M.-R. Kempton, S.E. Moran, C.V. Morley, V. Vuitton, Sulfur-driven haze formation in warm CO_2-rich exoplanet atmospheres, Nat. Astron. 4 (2020) 986–993, http://dx.doi.org/10.1038/s41550-020-1072-9.

[9] R. Hobbs, P.B. Rimmer, O. Shorttle, N. Madhusudhan, Sulfur chemistry in the atmospheres of warm and hot Jupiters, Mon. Not. R. Astron. Soc. 506 (2021) 3186–3204, http://dx.doi.org/10.1093/mnras/stab1839.

[10] A. Yachmenev, S.N. Yurchenko, T. Ribeyre, W. Thiel, High-level ab initio potential energy surfaces and vibrational energies of H_2CS, J. Chem. Phys. 135 (2011) 074302, http://dx.doi.org/10.1063/1.3624570.

[11] S. Erfort, M. Tschöpe, G. Rauhut, Toward a fully automated calculation of rovibrational infrared intensities for semi-rigid polyatomic molecules, J. Chem. Phys. 152 (2020) 244104, http://dx.doi.org/10.1063/5.0011832.

[12] H.-D. Meyer, F. Le Quéré, C. Léonard, F. Gatti, Calculation and selective population of vibrational levels with the multiconfiguration time-dependent hartree (MCTDH) algorithm, Chem. Phys. 329 (2006) 179–192, http://dx.doi.org/10.1016/j.chemphys.2006.06.002.

[13] S. Carter, N.C. Handy, The geometry and force field of thioformaldehyde, J. Mol. Spectrosc. 192 (1998) 263–267, http://dx.doi.org/10.1006/jmsp.1998.7692.

[14] J.M.L. Martin, J.P. Francois, R. Gijbels, The anharmonic force field of thioformaldehyde, H_2CS, by ab initio methods, J. Mol. Spectrosc. 168 (1994) 363–373, http://dx.doi.org/10.1006/jmsp.1994.1285.

[15] C. Léonard, G. Chambaud, P. Rosmus, S. Carter, N.C. Handy, The selective population of the vibrational levels of thioformaldehyde, Phys. Chem. Chem. Phys. 3 (2001) 508–513, http://dx.doi.org/10.1039/b008454i.

[16] S. Carter, A.R. Sharma, J.M. Bowman, P. Rosmus, R. Tarroni, Calculations of rovibrational energies and dipole transition intensities for polyatomic molecules using MULTIMODE, J. Chem. Phys. 131 (22) (2009) 224106, http://dx.doi.org/10.1063/1.3266577.

[17] J.-M. Flaud, W. Lafferty, A. Perrin, Y. Kim, H. Beckers, H. Willner, The first high-resolution analysis of the 10-μm absorption of thioformaldehyde, J. Quant. Spectrosc. Radiat. Transfer 109 (6) (2008) 995–1003, http://dx.doi.org/10.1016/j.jqsrt.2007.11.004.

[18] A. Maeda, I.R. Medvedev, M. Winnewisser, F.C. De Lucia, E. Herbst, H.S.P. Müller, M. Koerber, C.P. Endres, S. Schlemmer, High-frequency rotational spectrum of thioformaldehyde, H_2CS, in the ground vibrational state, Astrophys. J. Suppl. 176 (2008) 543–550, http://dx.doi.org/10.1086/528684.

[19] H.S.P. Müller, A. Maeda, S. Thorwirth, F. Lewen, S. Schlemmer, I.R. Medvedev, M. Winnewisser, F.C. De Lucia, E. Herbst, Laboratory spectroscopic study of isotopic thioformaldehyde, H_2CS, and determination of its equilibrium structure, Astron. Astrophys. 621 (2019) A143, http://dx.doi.org/10.1051/0004-6361/201834517.

[20] J.W.C. Johns, W.B. Olson, The infrared spectrum of thioformaldehyde, J. Mol. Spectrosc. 39 (1971) 479–505, http://dx.doi.org/10.1016/0022-2852(71)90219-0.

[21] T. Furtenbacher, A.G. Császár, J. Tennyson, An improved rovibrational linelist of formaldehyde, $H_2{}^{12}C^{16}O$, J. Mol. Spectrosc. 245 (2007) 115–125, http://dx.doi.org/10.1016/j.jms.2007.07.005.

[22] A.G. Császár, G. Czakó, T. Furtenbacher, E. Mátyus, An active database approach to complete rotational–vibrational spectra of small molecules, Annu. Rep. Comput. Chem. 3 (2007) 155–176, http://dx.doi.org/10.1016/s1574-1400(07)03009-5.

[23] T. Furtenbacher, A.G. Császár, J. Tennyson, The role of intensities in determining characteristics of spectroscopic networks, J. Molec. Struct. (THEOCHEM) 1009 (2012) 123–129, http://dx.doi.org/10.1016/j.molstruc.2011.10.057.

[24] R. Tóbiás, T. Furtenbacher, J. Tennyson, A.G. Császár, Accurate empirical rovibrational energies and transitions of $H_2{}^{16}O$, Phys. Chem. Chem. Phys. 21 (2019) 3473–3495, http://dx.doi.org/10.1039/c8cp05169k.

[25] J. Tennyson, S.N. Yurchenko, A.F. Al-Refaie, V.H.J. Clark, K.L. Chubb, E.K. Conway, A. Dewan, M.N. Gorman, C. Hill, A.E. Lynas-Gray, T. Mellor, L.K. McKemmish, A. Owens, O.L. Polyansky, M. Semenov, W. Somogyi, G. Tinetti, A. Upadhyay, I. Waldmann, Y. Wang, S. Wright, O.P. Yurchenko, The 2020 release of the ExoMol database: molecular line lists for exoplanet and other hot atmospheres, J. Quant. Spectrosc. Radiat. Transfer 255 (2020) 107228, http://dx.doi.org/10.1016/j.jqsrt.2020.107228.

[26] C.A. Bowesman, M. Shuai, S.N. Yurchenko, J. Tennyson, A high resolution line list for AlO, Mon. Not. R. Astron. Soc. 508 (2021) 3181–3193, http://dx.doi.org/10.1093/mnras/stab2525.

[27] A.R. Al-Derzi, S.N. Yurchenko, J. Tennyson, M. Melosso, N. Jiang, C. Puzzarini, L. Dore, T. Furtenbacher, R. Tobias, A.G. Császár, MARVEL analysis of the measured high-resolution spectra of formaldehyde, J. Quant. Spectrosc. Radiat. Transfer 266 (2021) 107563, http://dx.doi.org/10.1016/j.jqsrt.2021.107563.

[28] A.F. Al-Refaie, A. Yachmenev, J. Tennyson, S.N. Yurchenko, ExoMol line lists - VIII: A variationally computed line list for hot formaldehyde, Mon. Not. R. Astron. Soc. 448 (2015) 1704–1714, http://dx.doi.org/10.1093/mnras/stv091.

[29] I.E. Gordon, et al., The HITRAN 2020 molecular spectroscopic database, J. Quant. Spectrosc. Radiat. Transf. 277 (2022) 107949, http://dx.doi.org/10.1016/j.jqsrt.2021.107949.

[30] I. Snellen, High-dispersion spectroscopy of extrasolar planets: from CO in hot jupiters to O_2 in exo-earths, Philos. Trans. R. Soc. Lond. Ser. A Math. Phys. Eng. Sci. 372 (2014) 20130075, http://dx.doi.org/10.1098/rsta.2013.0075.

[31] J.L. Birkby, Spectroscopic direct detection of exoplanets, in: Handbook of Exoplanets, 2018, pp. 1485–1508.

[32] A.G. Császár, T. Furtenbacher, Spectroscopic networks, J. Mol. Spectrosc. 266 (2011) 99–103, http://dx.doi.org/10.1016/j.jms.2011.03.031.

[33] T. Furtenbacher, P. Árendás, G. Mellau, A.G. Császár, Simple molecules as complex systems, Sci. Rep. 4 (2014) 4654, http://dx.doi.org/10.1038/srep04654.

[34] P. Árendás, T. Furtenbacher, A.G. Császár, On spectra of spectra, J. Math. Chem. 54 (3) (2016) 806–822, http://dx.doi.org/10.1007/s10910-016-0591-1.

[35] J. Tennyson, P.F. Bernath, L.R. Brown, A. Campargue, M.R. Carleer, A.G. Császár, L. Daumont, R.R. Gamache, J.T. Hodges, O.V. Naumenko, O.L. Polyansky, L.S. Rothman, R.A. Toth, A.C. Vandaele, N.F. Zobov, A.Z. Fazliev, T. Furtenbacher, I.E. Gordon, S.N. Mikhailenko, B.A. Voronin, IUPAC critical evaluation of the rotational-vibrational spectra of water vapor. Part II. Energy levels and transition wavenumbers for $HD^{16}O$, $HD^{17}O$, and $HD^{18}O$, J. Quant. Spectrosc. Radiat. Transfer 111 (2010) 2160–2184, http://dx.doi.org/10.1016/j.jqsrt.2010.06.012.

[36] J. Tennyson, P.F. Bernath, L.R. Brown, A. Campargue, A.G. Császár, L. Daumont, R.R. Gamache, J.T. Hodges, O.V. Naumenko, O.L. Polyansky, L.S. Rothman, A.C. Vandaele, N.F. Zobov, A database of water transitions from experiment and theory (IUPAC technical report), Pure Appl. Chem. 86 (2014) 71–83, http://dx.doi.org/10.1515/pac-2014-5012.

[37] P.R. Bunker, P. Jensen, Molecular Symmetry and Spectroscopy, second ed., NRC Research Press, Ottawa, 1998.

[38] D.R. Johnson, F.X. Powell, Microwave detection of thioformaldehyde, Science 169 (1970) 679–680, http://dx.doi.org/10.1126/science.169.3946.679.

[39] Y. Beers, G.P. Klein, W.H. Kirchhoff, D.R. Johnson, Millimeter wave spectrum of thioformaldehyde, J. Mol. Spectrosc. 44 (1972) 553–557, http://dx.doi.org/10.1016/0022-2852(72)90263-9.

[40] B. Fabricant, D. Krieger, J.S. Muenter, Molecular beam electric resonance study of formaldehyde, thioformaldehyde, and ketene, J. Chem. Phys. 67 (1977) 1576–1586, http://dx.doi.org/10.1063/1.434988.

[41] D.J. Bedwell, G. Duxbury, Laser stark spectroscopy of thioformaldehyde in the 10-μm region: The ν_3, ν_4, and the ν_6 fundamentals, J. Mol. Spectrosc. 84 (1980) 531–558, http://dx.doi.org/10.1016/0022-2852(80)90042-9.

[42] P.H. Turner, L. Halonen, I.M. Mills, Fourier transform infrared spectra of H_2CS and D_2CS, J. Mol. Spectrosc. 88 (1981) 402–419, http://dx.doi.org/10.1016/0022-2852(81)90190-9.

[43] D. McNaughton, D.N. Bruget, Far-infrared and ν_2 vibration–rotation spectrum of thioformaldehyde and infrared spectrum of thioglyoxal, J. Mol. Spectrosc. 159 (1993) 340–349, http://dx.doi.org/10.1006/jmsp.1993.1132.

[44] D.J. Clouthier, G. Huang, A.G. Adam, A.J. Merer, Sub-doppler spectroscopy of thioformaldehyde: Excited state perturbations and evidence for rotation-induced vibrational mixing in the ground state, J. Chem. Phys. 101 (1994) 7300–7310, http://dx.doi.org/10.1063/1.468287.

[45] D.R. Johnson, F.X. Powell, W.H. Kirchhoff, Microwave spectrum, ground state structure, and dipole moment of thioformaldehyde, J. Mol. Spectrosc. 39 (1971) 136–145, http://dx.doi.org/10.1016/0022-2852(71)90284-0, URL https://www.sciencedirect.com/science/article/pii/0022285271902840.

[46] G. Winnewisser, A. Krupnov, M. Tretyakov, M. Liedtke, F. Lewen, A. Saleck, R. Schieder, A. Shkaev, S. Volokhov, Precision broadband spectroscopy in the Terahertz region, J. Mol. Spectrosc. 165 (1994) 294–300, http://dx.doi.org/10.1006/jmsp.1994.1132.

[47] D.T. Petkie, T.M. Goyette, R.P.A. Bettens, S.P. Belov, S. Albert, P. Helminger, F.C. De Lucia, A fast scan submillimeter spectroscopic technique, Rev. Sci. Instrum. 68 (4) (1997) 1675–1683, http://dx.doi.org/10.1063/1.1147970.

[48] C.M. Western, PGOPHER: A program for simulating rotational, vibrational and electronic spectra, J. Quant. Spectrosc. Radiat. Transfer 186 (2017) 221–242, http://dx.doi.org/10.1016/j.jqsrt.2016.04.010.

[49] S.N. Yurchenko, W. Thiel, P. Jensen, Theoretical ROVibrational energies (TROVE): A robust numerical approach to the calculation of rovibrational energies for polyatomic molecules, J. Mol. Spectrosc. 245 (2007) 126–140, http://dx.doi.org/10.1016/j.jms.2007.07.009.

[50] T. Mellor, A. Owens, S.N. Yurchenko, J. Tennyson, ExoMol line lists – XLVIII. Rvibronic molecular line list for thioformaldehyde (H_2CS), Mon. Not. R. Astron. Soc.

[51] C.P. Endres, S. Schlemmer, P. Schilke, J. Stutzki, H.S.P. Müller, The cologne database for molecular spectroscopy, CDMS, in the virtual atomic and molecular data centre, VAMDC, J. Mol. Spectrosc. 327 (2016) 95–104, http://dx.doi.org/10.1016/j.jms.2016.03.005.